Extended model for control of thermal energy in buildings

Ashish Bhattarai, Zahir Barahmand, Sina Orangi, Bernt Lie

University of South-Eastern Norway, Porsgrunn, Norway, Bernt.Lie@usn.no

Abstract

The paper extends a previous model of a heated water system with stratification, with an external floor heating circulation loop and a detailed model of heat transfer from water pipe to heated room. A minor error in the previous stratification model is corrected. The floor heating loop is posed as a cross-current heat exchanger, and a simple approximation of time delay for heat advection is suggested. For heat flow to the room, infinitely fast heating of an aluminum plate is suggested, with slower heat transfer to chip-board, through fiberboard and parquet to the room. The room is heated by a combination of convection and radiation. The results show that the inclusion of the heat circulation loop shows that this has an important effect on the dynamics of the system, and that this loop should be taken into account if parameters are tuned to fit the model to experimental data.

Keywords: floor heating, energy in buildings, energy storage, hot water tank model, water distribution system, stratified flow model

1 Introduction

Floor heating has been used for thousands of years, and essentially consists of a heat generation system and a heat distribution system with heat transfer through the floor. Modern studies of low energy buildings focus on taking advantage of water with low thermal value (lukewarm, 30–35 °C), which necessitates reducing heat transfer coefficients in the system. Modern control systems allow for reducing the temperature when (part of) the building is unused, but require heating system with low heat capacity to be efficient. This implies using above-floor systems, i.e., inserting pipes in the underlayment between the subfloor (e.g., chipboard) and the floor covering (parquet, etc.).

(Lie et al., 2014) discussed the use of solar heating assisted by electric heating for floor heating, and studied the use of Model Predictive Control (MPC), and (Lie, 2015) discussed a minor improvement of the heater model. In (Johansen et al., 2019), an improved model of an electric heater was considered, and compared with experimental data. Specifically, a model of stratification due to (Viskanta et al., 1977) was used, see also (Xu et al., 2014). (Lago et al., 2019) discusses a similar model, and a possible smooth description of the buoyancy conductivity. A more complex model of stratification is given in (Vrettos, 2016), with a two stage diffusion predictor and buoyancy corrector step. A system with some details of floor heating is discussed in (Ho et al., 1995).

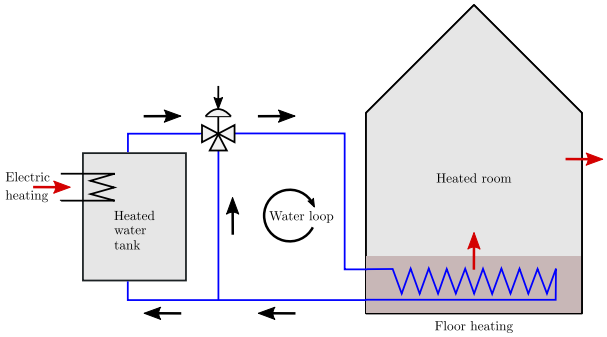

Figure 1. Floor heating system.

In this paper, the heated water tank model as in (Johansen et al., 2019) is corrected for missing constants, and is extended with a water distribution system for floor heating. The system is extended to include a circulation loop for floor heating — with more details about the floor layers than in (Lie et al., 2014), while excluding the solar heating. The effect of the circulation loop is examined; this circulation loop was not included in the model fitting of (Johansen et al., 2019). The paper is organized as follows. In Section 2, an overview is given of the system. In Section 3, the dynamic model of the system with heater, water circulation, and floor layers + room is developed. In Section 4, some simulations results are given, while conclusions are drawn in Section 5.

2 System overview

2.1 Floor heating

Consider a floor heating system for a building, Fig. 1.

The system consists of an electrically heated, stratified water tank which supplies heated water to a water loop passing through water pipes embedded in the floor. The heated floor then provides heating to the room above to compensate for heat loss to the surroundings. Both floor temperature and air temperature in the heated room is of importance for inhabitant comfort. Typically, a floor temperature of ca. 22 °C and an air temperature of ca. 20 °C is deemed optimal when in use.

The heated water tank is influenced by external signals in the form of the loop volumetric water flow rate $\dot{V}_\ell$, the split range valve signal u_v which determines how much water goes through the heated tank, the ambient temperature of the heated tank, T_a^t, and the fraction of full electric power u_P that is used to heat the tank. In the model of (Jo-

hansen et al., 2019), the inlet temperature T_i at the bottom of the tank was also an external signal; in this work, T_i is a signal that comes from the heated floor subsystem, and is thus not a free, external input.

The water from the heated tank flows into the water loop at temperature T_i^ℓ (the temperature after the split range valve of the heated tank), and passes through a lengthy pipe embedded in the floor. The floor pipe is essentially a heat exchanger for transfer of heat to the floor. From the floor, heat is transferred to the room by convection and radiation. Finally, the room experiences a heat loss to the surroundings which is at external ambient temperature T_a^r.

2.2 Heated water tank: modification

The stratified heated water tank with discretization is given in detail in Johansen et al. (2019). In (Johansen et al., 2019), buoyant turbulent mixing flux $\dot{Q}''_\mathrm{db}$ was correctly given by

$$\frac{\partial \dot{Q}''_\mathrm{db}}{\partial z} = -k_\mathrm{b}\frac{\partial^2 T}{\partial z^2}.$$

Here, z is vertical position, k_b is a buoyancy conductivity, and T is the temperature distribution over z . However, here we correct the expression for k_b, which should be

$$k_\mathrm{b} = \begin{cases} \rho\hat{c}_p \cdot \kappa^2 d^2 \sqrt{g\alpha_p \left|\frac{\partial T}{\partial z}\right|}, & \frac{\partial T}{\partial z} < 0 \\ 0, & \frac{\partial T}{\partial z} \geq 0, \end{cases}$$

where ρ is density, $\hat{c}_p$ is specific heat capacity, κ is the von Kármán constant, d is the tank diameter, g is acceleration of gravity, and α_p is the thermal expansion coefficient at constant pressure.

The essential difference is that in the previous publication, $\rho\hat{c}_p$ was replaced by an ad hoc tuning parameter c_b which was suggested to have a value near unity.

2.3 Transport of water in pipes

If we assume that the pipes transporting water to and from the heated floor are perfectly insulated, the temperature for these stretches are given by the advection equation:

$$\frac{\partial T}{\partial t} = -v\frac{\partial T}{\partial x}$$

where

$$v = \frac{\dot{V}_\ell}{A_\mathrm{p}}$$

with $\dot{V}_\ell$ the volumetric flow rate in the water loop through the floor heating system, and A_p the cross sectional area of the pipe. The advection model has the well known solution

$$T(t, x = L) = T\left(t - \frac{L}{v}, x = 0\right)$$

where L is the length of the pipe. The Laplace transform of this solution is

$$T(s, x = L) = \exp\left(-\frac{L}{v}s\right) T(s, x = 0).$$

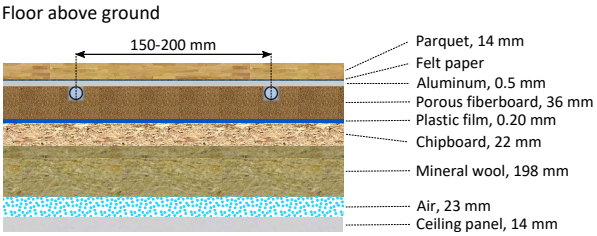

Figure 2. Structure of floor heating (not to scale), freely after https://www.uponor.no/vvs/produkter/gulvvarme/calma-trinnlydplater. Water flows in water pipes, which typically are separated by 150–200 mm.

This time delay can be expressed directly in some modeling languages. In Modelica, the syntax would be[1]:

```
TxL = delay(Tx0, L/v)
```

Other languages, such as Julia, have special solvers for delay differential equations.

Introducing $\tau \equiv \frac{L}{v}$ as the time delay, we can approximate the solution by N compartments. With partial delay τ_i such that $\sum_{i=1}^N \tau_i = \tau$, a possible Padé approximation is

$$\frac{T(s; x = L)}{T(s; x = 0)} = \frac{1}{\exp(\tau_N s)} \prod_{i=1}^{N-1} \frac{\exp\left(-\frac{\tau_i}{2}s\right)}{\exp\left(\frac{\tau_i}{2}s\right)} \approx \frac{1}{1+\tau_N s} \prod_{i=1}^{N-1} \frac{1-\frac{\tau_i}{2}s}{1+\frac{\tau_i}{2}s}$$

with realization

$$\begin{aligned} \frac{\mathrm{d}x_1}{\mathrm{d}t} &= \frac{1}{\tau_1}(T_{x=0} - x_1) \\ \frac{\mathrm{d}x_1}{\mathrm{d}t} + \frac{\mathrm{d}x_2}{\mathrm{d}t} &= \frac{2}{\tau_2}(x_1 - x_2) \\ &\vdots \\ \frac{\mathrm{d}x_{N-1}}{\mathrm{d}t} + \frac{\mathrm{d}x_N}{\mathrm{d}t} &= \frac{2}{\tau_N}(x_{N-1} - x_N) \end{aligned}$$

where $T_{x=L} = x_N$. An advection model/time delay has non-minimum phase characteristics (Åstrøm and Murray, 2008), and the all-pass terms $\frac{1-\frac{\tau_i}{2}s}{1+\frac{\tau_i}{2}s}$ ensures that the non-minimum phase characteristic is retained. At the same time, the lag term $\frac{1}{1+\tau_N s}$ ensures that the time derivative of the input signal $T_{x=0}$ can be avoided. This advection model approximation constitutes a DAE, which can easily be changed into an ODE. However, the resulting ODE becomes more complicated, and if we use a DAE solver, such a reformulation is not needed.

2.4 Heat transfer from water to floor

2.4.1 Structure of heated floor

The structure of the floor layers is depicted in Fig. 2.

Water pipes of PEX (cross-linked polyethylene) are put in grooves in the *underlayment*, typically in flexible, porous fiberboard which also serves to dampen the sound

[1] https://www.openmodelica.org/forum/default-topic/1907-how-to-make-a-time-delay,-w-t-r

of steps. To secure good heat transfer to the *floor finish* (e.g., parquet), the pipes are put in thermal contact with an aluminum plate which has high thermal conductivity, and thus spreads the heat evenly in the aluminum plate. The water pipes are either surrounded (50-75%) by Ω-plates or clips, or they are surrounded by a plaster with good thermal conductivity such as *anhydrite* — this is to secure the best possible heat transfer area to the aluminum plate.

To achieve even temperature in the aluminum plate and thus in the floor finish (e.g., parquet), pipes of outer diameter 12–20 mm and 2 mm wall thickness of PEX are typically put at a distance of 15–20 cm along the entire floor. Between the floor finish and the aluminum plate is felt paper, or similar, to enable some sliding between the floor finish and the underlayment and thus reduce sounds of movement.

The floor layer structure in Fig. 2 is common when there is a room below the floor. We will neglect heat transfer resistance in the very thin plastic film and felt paper. For simplicity, we will also assume that the insulation (mineral wool) is perfect, and that there is no heat leakage to the room below.

2.4.2 Heat transfer from water to aluminum

To simplify the model, we assume a fast heat transfer between water and aluminum, and due to aluminum's high heat conduction, the aluminum temperature is taken to be homogeneous. Heat transfer can then be modeled as in a steady state cross current heat exchanger. The water temperature is at the tube side (pipe), with temperature $T_\mathrm{p}(x)$ varying along the pipe length, while aluminum is the shell side with temperature T_al being independent of position.

Introducing the tube side water pipe dimensionless *Stanton* number N_St^p,

$$N_\mathrm{St}^\mathrm{p} = \frac{\mathscr{U}_\mathrm{x} A_\mathrm{x}}{\dot{m}_\mathrm{p} \hat{c}_{p,\mathrm{w}}},$$

with heat transfer coefficient $\mathscr{U}_\mathrm{x}$, contact surface A_x in heat exchanger, tube side (water) mass flow rate $\dot{m}_\mathrm{p}$, and tube side heat capacity $\hat{c}_{p,\mathrm{w}}$, and assuming N_St^p is independent of position x, we find the heat transfer from tube side water *pipe* to shell side *aluminum* $\dot{Q}_\mathrm{p2al}$ to be

$$\dot{Q}_\mathrm{p2al} = \dot{m}_\mathrm{p} \hat{c}_{p,\mathrm{w}} \left[1 - \exp\left(-N_\mathrm{St}^\mathrm{p}\right)\right] \left(T_\mathrm{i}^\mathrm{p} - T_\mathrm{al}\right).$$

Here, T_i^p is the water pipe inlet temperature to the "heat exchanger", while T_al is the exit temperature of the shell side = aluminum temperature.

The aluminum (shell side) temperature is given by the energy balance for the shell side (aluminum). Since the heat conduction in aluminum is fast, we will assume steady state for aluminum, i.e.,

$$0 = \frac{\mathrm{d}U_\mathrm{al}}{\mathrm{d}t} = \dot{Q}_\mathrm{p2al} - \dot{Q}_\mathrm{al2x},$$

where U_al is the internal energy of the shell side (aluminum), $\dot{Q}_\mathrm{al2x}$ is the combined heat flow to the fiberboard and the parquet. We will return to an expression for $\dot{Q}_\mathrm{al2x}$.

We also need the effluent water (tube side) temperature T_e^p, which is the temperature of the water returning to the heated tank:

$$T_\mathrm{e}^\mathrm{p} = T_\mathrm{al} + \exp\left(-N_\mathrm{St}^\mathrm{p}\right)\left(T_\mathrm{i}^\mathrm{p} - T_\mathrm{al}\right). \tag{1}$$

In the expression for the Stanton number,

$$\dot{m}_\mathrm{p} = \dot{V}_\ell \rho_\mathrm{w}$$
$$\frac{1}{\mathscr{U}_\mathrm{x}} = \frac{1}{h_\mathrm{w}} + \frac{\frac{d_\mathrm{p}}{2}\ln\left(1 + \frac{2\delta_\mathrm{p}}{d_\mathrm{p}}\right)}{k_\mathrm{p}}$$

where h_w is the heat transfer coefficient for water to solid in the pipe, d_p is the inner diameter of the pipe, δ_p is the thickness of the plastic water pipe wall, and k_p is thermal conductivity of the pipe material (plastic) (Lydersen, 1979).

Likewise, the contact area A_x is, say, 75% of the plastic pipe surface, i.e.,

$$A_\mathrm{x} = 0.75 \cdot \pi \left(d_\mathrm{p} + 2\delta_\mathrm{p}\right) L_\mathrm{f}$$

where d_p is the inner diameter of the pipe, while L_f is the length of the pipe in contact with the shell side (aluminum) in the *floor*.

2.4.3 Heat transfer to plates

Steady energy balance for the aluminum plate leads to

$$\dot{Q}_\mathrm{p2al} = \dot{Q}_\mathrm{al2x} = \dot{Q}_\mathrm{al2pq} + \dot{Q}_\mathrm{al2fb}$$

where $\dot{Q}_\mathrm{al2pq}$ is the heat transfer from aluminum at temperature T_al to parquet, while $\dot{Q}_\mathrm{al2fb}$ is the heat transfer from aluminum to fiberboard. In addition to this, we will also need the heat transfer $\dot{Q}_\mathrm{fb2cb}$ from fiberboard to chipboard.

The dynamics of parquet, fiberboard, and chipboard will be considerably slower than that of aluminum, so we include a dynamic model of these plates. In a simplified description, we assume a thin boundary layer near aluminum for parquet and fiberboard, and a thin boundary layer near fiberboard for chipboard — for the rest of the board volumes, we assume homogeneous temperature T. This leads to a simplified model

$$\rho A \hat{c}_p \delta \frac{\mathrm{d}T}{\mathrm{d}t} = A\frac{k}{\delta}\left(T_0 - T\right) - \dot{Q}_{x=\delta}.$$

Applying this model to all three boards, we associate quantities as in Table 1. In Table 1, $\dot{Q}_\mathrm{pq2r}$ is the heat flow from the parquet to the room — which consists of convective heat flow and radiative heat flow. $\dot{Q}_\mathrm{fb2cb}$ is the heat flow from the fiberboard to the chipboard. Finally, the heat flow out of the chipboard is zero, because we have assumed that the insulation material below the chipboard ("mineral wool") is perfect.

Table 1. Quantities and flow rates for boards.

Quantity	Parquet	Fiberboard	Chipboard
T	T_{pq}	T_{fb}	T_{cb}
δ	δ_{pq}	δ_{fb}	δ_{cb}
T_0	T_{al}	T_{al}	T_{fb}
$\dot{Q}_{x=\delta}$	$\dot{Q}_{\mathrm{pq2r}}$	$\dot{Q}_{\mathrm{fb2cb}}$	0

2.5 Heat transfer related to room

The heat transferred into the room from the parquet floor, $\dot{Q}_{\mathrm{pq2r}}$, consists of heat convection from the floor, $\dot{Q}^{\mathrm{c}}_{\mathrm{pq2r}}$, and net radiation, $\dot{Q}^{\mathrm{r}}_{\mathrm{pq2r}}$. Heat convection is given by floor area A_{pq} and heat flux $\dot{Q}''^{,\mathrm{c}}_{\mathrm{pq2r}}$,

$$\dot{Q}''^{,\mathrm{c}}_{\mathrm{pq2r}} = \mathscr{U}_{\mathrm{pq2r}} \left(T_{\mathrm{pq}} - T_{\mathrm{r}}\right).$$

The net radiation consists of radiation out due to parquet floor temperature, and return radiation due to radiation from the ceiling. Assuming that the ceiling has the same temperature as the room air T_{r}, it can be shown that

$$\dot{Q}''^{,\mathrm{r}}_{\mathrm{pq2r}} = \frac{1}{\frac{1}{\varepsilon_{\mathrm{pq}}} + \frac{1}{\varepsilon_{\mathrm{r}}} - 1} \sigma \left(T^4_{\mathrm{pq}} - T^4_{\mathrm{r}}\right)$$

where σ is Stefan-Boltzmann's constant, and $\varepsilon_{\mathrm{pq}}$ and ε_{r} are the emissivities from the parquet floor and the room (ceiling), respectively. In this radiation expression, absolute temperature must be used. The expression is based on radiation between two parallel planes. In summary,

$$\dot{Q}_{\mathrm{pq2r}} = A_{\mathrm{pq}} \left(\dot{Q}''^{,\mathrm{c}}_{\mathrm{pq2r}} + \dot{Q}''^{,\mathrm{r}}_{\mathrm{pq2r}}\right).$$

There is also a convective heat loss to the surroundings, $\dot{Q}_{\mathrm{r2a}}$, given by

$$\dot{Q}_{\mathrm{r2a}} = A_{\mathrm{r}} \dot{Q}''_{\mathrm{r2a}}$$

where A_{r} is the net surface between the room and the ambient of the room, while

$$\dot{Q}''_{\mathrm{r2a}} = \mathscr{U}_{\mathrm{r2a}} \left(T_{\mathrm{r}} - T^{\mathrm{r}}_{\mathrm{a}}\right).$$

3 Dynamic model

Since the density of water and air will be assumed constant, we essentially need the energy balance. The model can be summarized as follows.

3.1 Heated tank

The model from (Johansen et al., 2019) has been corrected in a project in a course at USN[2], as described in Section 2.2. For model details, see (Johansen et al., 2019).

[2]University of South-Eastern Norway: Course FM1015 Modelling of Dynamic Systems, group project Fall of 2019.

3.2 Floor heating/heat exchanger

If we neglect the time delay from the heated tank to the inlet to the floor coil pipes, we have $T^{\mathrm{p}}_{\mathrm{i}}(t) = T^{\ell}_{\mathrm{i}}(t)$. If we instead include the time delay, we have $T^{\mathrm{p}}_{\mathrm{i}}(t) = T^{\ell}_{\mathrm{i}}(t - \tau_{\mathrm{t2f}})$ where the time delay from the heater to the floor is $\tau_{\mathrm{t2f}} = \frac{L_{\mathrm{t2f}}}{v} = \frac{L_{\mathrm{t2f}}}{\dot{V}_{\ell}/A_{\mathrm{p}}}$ with length L_{t2f} of the water pipe from the heated tank to the floor coil inlet, volumetric flow rate $\dot{V}_{\ell}$ in the floor heating pipes, and cross sectional area A_{p} of the pipe, i.e., $A_{\mathrm{p}} = \pi r^2_{\mathrm{p}} = \pi d^2_{\mathrm{p}}/4$.

With aluminum plate temperature T_{al}, the effluent temperature $T^{\mathrm{p}}_{\mathrm{e}}$ of the water after the floor has been heated is then

$$T^{\mathrm{p}}_{\mathrm{e}} = T_{\mathrm{al}} + \exp\left(-N^{\mathrm{p}}_{\mathrm{St}}\right)\left(T^{\mathrm{p}}_{\mathrm{i}} - T_{\mathrm{al}}\right),$$

where the tube (pipe) side dimensionless *Stanton* number $N^{\mathrm{p}}_{\mathrm{St}}$ is

$$N^{\mathrm{p}}_{\mathrm{St}} = \frac{(\mathscr{U}A)_{\mathrm{x}}}{\dot{m}_{\mathrm{p}} \hat{c}_{p,\mathrm{w}}},$$

with overall heat transfer coefficient $\mathscr{U}_{\mathrm{x}}$, contact surface A_{x} in heat exchanger, water mass flow rate in the pipes $\dot{m}_{\mathrm{p}}$, and water heat capacity $\hat{c}_{p,\mathrm{w}}$, and assuming $N^{\mathrm{p}}_{\mathrm{St}}$ is independent of position x. Here, the overall heat transfer coefficient is given by

$$\frac{1}{\mathscr{U}_{\mathrm{x}}} = \frac{1}{h_{\mathrm{w}}} + \frac{\frac{d_{\mathrm{p}}}{2} \ln\left(1 + \frac{2\delta_{\mathrm{p}}}{d_{\mathrm{p}}}\right)}{k_{\mathrm{p}}}$$

where h_{w} is the heat transfer coefficient from water to pipe wall, k_{p} is the conductivity of the pipe wall (plastic), d_{p} is the inner pipe diameter, while δ_{p} is the pipe thickness. The contact surface A_{x} is assumed to be 75% of the external surface of the pipes, i.e.,

$$A_{\mathrm{x}} = 0.75\pi \left(d_{\mathrm{p}} + 2\delta_{\mathrm{d}}\right) L_{\mathrm{f}}.$$

The heat transferred from water pipe (tube side) to aluminum (shell side) is then $\dot{Q}_{\mathrm{p2al}}$ given by

$$\dot{Q}_{\mathrm{p2al}} = \dot{m}_{\mathrm{p}} \hat{c}_{p,\mathrm{w}} \left[1 - \exp\left(-N^{\mathrm{p}}_{\mathrm{St}}\right)\right]\left(T^{\mathrm{p}}_{\mathrm{i}} - T_{\mathrm{al}}\right).$$

Here, $T^{\mathrm{p}}_{\mathrm{i}}$ is the water pipe inlet temperature to the "heat exchanger", while T_{al} is the exit temperature of the shell side; since the shell side is assumed to have homogeneous, T_{al} is the aluminum temperature.

The water temperature that enters the return loop to the heated tank is $T^{\mathrm{p}}_{\mathrm{e}}(t)$ if we neglect time delay, and $T^{\mathrm{p}}_{\mathrm{e}}(t - \tau_{\mathrm{f}})$ if we include the time delay of the water flowing through the floor coils, $\tau_{\mathrm{f}} = \frac{L_{\mathrm{f}}}{v} = \frac{L_{\mathrm{f}}}{\dot{V}_{\ell}/A_{\mathrm{p}}}$ (assuming the same pipe cross sectional area everywhere).

Assuming steady energy balance for the aluminum plate gives

$$0 = \dot{Q}_{\mathrm{p2al}} - \dot{Q}_{\mathrm{al2x}},$$

where $\dot{Q}_{\mathrm{p2al}}$ is given above, while $\dot{Q}_{\mathrm{al2x}}$ is given by

$$\dot{Q}_{\mathrm{al2x}} = \dot{Q}_{\mathrm{al2pq}} + \dot{Q}_{\mathrm{al2fb}}$$

with

$$\dot{Q}_{\mathrm{al2pq}} = A_{\mathrm{r}} \frac{k_{\mathrm{pq}}}{\delta_{\mathrm{pq}}} \left(T_{\mathrm{al}} - T_{\mathrm{pq}}\right)$$

and

$$\dot{Q}_{\mathrm{al2fb}} = A_{\mathrm{r}} \frac{k_{\mathrm{fb}}}{\delta_{\mathrm{fb}}} \left(T_{\mathrm{al}} - T_{\mathrm{fb}}\right)$$

with A_{r} being the area of the room floor.

For the heat flow from fiberboard to chipboard, we have

$$\dot{Q}_{\mathrm{fb2cb}} = A_{\mathrm{r}} \frac{k_{\mathrm{cb}}}{\delta_{\mathrm{cb}}} \left(T_{\mathrm{fb}} - T_{\mathrm{cb}}\right).$$

The effluent water from floor heating at temperature $T_{\mathrm{e}}^{\mathrm{p}}$ is returned to the heated tank through a pipe of length L_{f2t}. If the time delay is neglected, we have $T_{\mathrm{i}}(t) = T_{\mathrm{e}}^{\mathrm{p}}(t)$. If we include the time delay, the relation is $T_{\mathrm{i}}(t) = T_{\mathrm{e}}^{\mathrm{p}}\left(t - \tau_{\mathrm{f2p}}\right)$ where $\tau_{\mathrm{f2p}} = \frac{L_{\mathrm{f2p}}}{\dot{V}_\ell / A_{\mathrm{p}}}$.

3.3 Board models

The models for the parquet, the fiberboard and the chipboard can be summarized as follows:

$$\rho_{\mathrm{pq}} A_{\mathrm{r}} \hat{c}_{p,\mathrm{pq}} \delta_{\mathrm{pq}} \frac{\mathrm{d}T_{\mathrm{pq}}}{\mathrm{d}t} = \dot{Q}_{\mathrm{al2pq}} - \dot{Q}_{\mathrm{pq2r}}$$
$$\rho_{\mathrm{fb}} A_{\mathrm{r}} \hat{c}_{p,\mathrm{fb}} \delta_{\mathrm{fb}} \frac{\mathrm{d}T_{\mathrm{fb}}}{\mathrm{d}t} = \dot{Q}_{\mathrm{al2fb}} - \dot{Q}_{\mathrm{fb2cb}}$$
$$\rho_{\mathrm{cb}} A_{\mathrm{r}} \hat{c}_{p,\mathrm{cb}} \delta_{\mathrm{cb}} \frac{\mathrm{d}T_{\mathrm{cb}}}{\mathrm{d}t} = \dot{Q}_{\mathrm{fb2cb}}.$$

Here,

$$\dot{Q}_{\mathrm{pq2r}} = \dot{Q}^{\mathrm{c}}_{\mathrm{pq2r}} + \dot{Q}^{\mathrm{r}}_{\mathrm{pq2r}}$$
$$\dot{Q}^{\mathrm{c}}_{\mathrm{pq2r}} = A_{\mathrm{r}} \mathscr{U}_{\mathrm{pq2r}} \left(T_{\mathrm{pq}} - T_{\mathrm{r}}\right)$$
$$\dot{Q}^{\mathrm{r}}_{\mathrm{pq2r}} = A_{\mathrm{r}} \frac{1}{\frac{1}{\varepsilon_{\mathrm{pq}}} + \frac{1}{\varepsilon_{\mathrm{r}}} - 1} \sigma \left(T_{\mathrm{pq}}^4 - T_{\mathrm{r}}^4\right).$$

3.4 Room model

With a simplistic room model, we only consider air mass m_{r} with no ventilation. Then

$$\frac{\mathrm{d}U_{\mathrm{r}}}{\mathrm{d}t} = \dot{Q}_{\mathrm{pq2r}} - \dot{Q}_{\mathrm{r2a}}$$

where U_{r} is the internal energy of the room air, for simplicity, $\mathrm{d}U_{\mathrm{r}} \approx m_{\mathrm{r}} \hat{c}_{v,\mathrm{a}} \mathrm{d}T_{\mathrm{r}}$, where $\hat{c}_{v,\mathrm{a}} = \hat{c}_{p,\mathrm{a}} - \frac{R}{M_{\mathrm{a}}}$ is the specific heat capacity of air at constant volume, $\hat{c}_{p,\mathrm{a}}$ is the specific heat capacity at constant pressure, with gas constant R and molar mass of air M_{a}. Here,

$$\dot{Q}_{\mathrm{r2a}} = A_{\mathrm{r}}^{\mathrm{s}} \mathscr{U}_{\mathrm{r}} \left(T_{\mathrm{r}} - T_{\mathrm{a}}^{\mathrm{r}}\right)$$

where $A_{\mathrm{r}}^{\mathrm{s}}$ is the surface area of the room against the ambient temperature $T_{\mathrm{a}}^{\mathrm{r}}$, $\mathscr{U}_{\mathrm{r}}$ is the overall heat transfer coefficient from room air temperature T_{r} to ambient temperature.

In a more realistic room model, we would also take into account stored energy in furniture, walls, etc., multiple rooms with transport between the rooms, and radiation from the sun into the room.

3.5 Model parameters

Model parameters for the heated tank are given in (Johansen et al., 2019), while model parameters for the floor/heated room are given in Table 2.

Let us briefly discuss the time delays of water flow in the system. With $\dot{V}_\ell \in [1, 13]\,\mathrm{L/min}$ and $A_{\mathrm{p}} = \pi d_{\mathrm{p}}^2/4$ we find time delays:

$$\tau_{\mathrm{t2f}} = \frac{L_{\mathrm{t2f}}}{\dot{V}_\ell / A_{\mathrm{p}}} = \frac{20 \cdot 10^1 \pi \frac{\left(12 \cdot 10^{-2}\right)^2}{4}}{\dot{V}_\ell} = \frac{2.26}{\dot{V}_\ell} = [0.17, 2.3]\,\mathrm{min}$$
$$\tau_{\mathrm{f}} = \frac{L_{\mathrm{f}}}{\dot{V}_\ell / A_{\mathrm{p}}} = \frac{250}{\dot{V}_\ell \pi \frac{\left(12 \cdot 10^{-2}\right)}{4}} = [2.2, 28.3]\,\mathrm{min}$$
$$\tau_{\mathrm{f2t}} = \frac{L_{\mathrm{f2t}}}{\dot{V}_\ell / A_{\mathrm{p}}} = \tau_{\mathrm{t2f}}.$$

This means that for low flow rates, the time delay main be up to 30 min through the floor pipe. The time delay in the transport pipes is small, though. The characteristic time constants of the system are in the same order of magnitude, (Johansen et al., 2019). Thus, the time delay should be considered. For simplicity, a simple approximation of the time delay is to put it between the outlet of the floor pipe and the heated tank. We use the approximate description

$$\frac{\mathrm{d}x_1}{\mathrm{d}t} = \frac{1}{\tau_1}\left(T_{\mathrm{e}}^{\mathrm{p}} - x_1\right)$$
$$\frac{\mathrm{d}x_1}{\mathrm{d}t} + \frac{\mathrm{d}x_2}{\mathrm{d}t} = \frac{2}{\tau_2}\left(x_1 - x_2\right)$$
$$\vdots$$
$$\frac{\mathrm{d}x_{N-1}}{\mathrm{d}t} + \frac{\mathrm{d}x_N}{\mathrm{d}t} = \frac{2}{\tau_N}\left(x_{N-1} - x_N\right)$$

with $T_{\mathrm{i}} = x_N$ and $\tau = \sum_{i=1}^{N} \tau_i = \frac{(L_{\mathrm{t2f}} + L_{\mathrm{f}} + L_{\mathrm{f2t}}) A_{\mathrm{p}}}{\dot{V}_\ell}$. For simplicity, we set $\tau_i = \frac{\tau}{N}$.

4 Simulation results

The model of the heated tank with 20 slices and specified input temperature T_{i} is simulated, and compared to a model of the combined heated tank and floor heating with circulating water providing T_{i}, using the model parameters in (Johansen et al., 2019) and those in Table 2, with $N = 3$ "volumes" in the time delay approximation.

Key inputs to the systems are given in Fig. 3. Observe that inlet temperature to the heated tank, T_{i}, is only used when the heated tank is simulated as an independent system. It has been assumed that the ambient temperature to the heated tank is $T_{\mathrm{a}}^{\mathrm{t}} = 15\,^\circ\mathrm{C}$, while that the outdoor temperature is $T_{\mathrm{a}}^{\mathrm{r}} = 5\,^\circ\mathrm{C}$; both are assumed to be constant over time.Initial values of all states (temperatures) are set to $25\,^\circ\mathrm{C}$.

Figure 4 compares the temperature distribution in the heated tank for the cases (a) that the heated tank is an independent system with specified T_{i}, and (b) that the heated

Table 2. Model parameters for room with floor heating.

Parameter	Value	Comment
d_p	$12\,\mathrm{mm}$	Inner diameter of floor pipe
δ_p	$2\,\mathrm{mm}$	Thickness of floor pipe wall
k_p	$0.5\,\mathrm{W/m\,K}$	Thermal conductivity of floor pipe material (PEX)
L_f	$250\,\mathrm{m}$	Length of pipe in floor heat exchanger
L_t2f	$20\,\mathrm{m}$	Length of pipe from tank to floor coils
L_f2t	$20\,\mathrm{m}$	Length of return pipe from floor coils to tank
A_x	$0.75\pi\left(d_\mathrm{p}+2\delta_\mathrm{p}\right)L_\mathrm{f}$	Heat transfer area from water to aluminum plate
h_w	$6500\,\mathrm{W/m^2K}$	Heat transfer from water to pipe wall
$\mathscr{U}_\mathrm{x}$	$1/\left(\frac{1}{h_\mathrm{w}}+\frac{\frac{d_\mathrm{p}}{2}\ln\left(1+\frac{2\delta_\mathrm{p}}{d_\mathrm{p}}\right)}{k_\mathrm{p}}\right)$	Overall heat transfer coefficient, water to aluminum
A_r	$50\,\mathrm{m^2}$	Area of floor with floor heating
h_r	$2.5\,\mathrm{m}$	Height of room
V_r	$h_\mathrm{r}A_\mathrm{r}$	Volume of room
ρ_a	$1.225\,\mathrm{kg/m^3}$	Density of air
$\hat{c}_{p,\mathrm{a}}$	$1\,\mathrm{kJ/kg\,K}$	Specific heat capacity at constant pressure, air
R	$8.31\,\mathrm{kJ/kmol\,K}$	Gas constant
M_a	$28.97\,\mathrm{kg/kmol}$	Molar mass of air
$\hat{c}_{v,\mathrm{a}}$	$\hat{c}_{p,\mathrm{a}}-\frac{R}{M_\mathrm{a}}$	Specific heat capacity at constant volume, air
m_r	$\rho_\mathrm{a}V_\mathrm{r}$	Mass of air in room
δ_pq	$14\,\mathrm{mm}$	Thickness of parquet
δ_fb	$36\,\mathrm{mm}$	Thickness of fiberboard
δ_cb	$22\,\mathrm{mm}$	Thickness of chipboard
ρ_pq	$750\,\mathrm{kg/m^3}$	Density of parquet material
ρ_fb	$230\,\mathrm{kg/m^3}$	Density of fibreboard material
ρ_cb	$700\,\mathrm{kg/m^3}$	Density of chipboard material
$\hat{c}_{p,\mathrm{pq}}$	$2\,\mathrm{kJ/kg\,K}$	Specific heat capacity of parquet material
$\hat{c}_{p,\mathrm{fb}}$	$1.4\,\mathrm{kJ/kg\,K}$	Specific heat capacity of fibreboard material
$\hat{c}_{p,\mathrm{cb}}$	$1.8\,\mathrm{kJ/kg\,K}$	Specific heat capacity of chipboard matierial
k_pq	$0.17\,\mathrm{W/m\,K}$	Thermal conductivity of parquet material
k_fb	$0.049\,\mathrm{W/m\,K}$	Thermal conductivity of fibreboard material
k_cb	$0.15\,\mathrm{W/m\,K}$	Thermal conductivity of chipboard material
σ	$5.6494\cdot10^{-8}\,\frac{\mathrm{W}}{\mathrm{K^4\,m^2}}$	Stefan-Boltmann's constant
ε_pq	$0.9-$	Emissivity of parquet
ε_r	$0.96-$	Emissivity of ceiling (room)
A_r^s	$A_\mathrm{r}+4h_\mathrm{r}\sqrt{A_\mathrm{r}}$	Surface area of room
$\frac{k_\mathrm{r}}{\delta_\mathrm{r}}$	$0.15\,\mathrm{W/m^2K}$	Heat transfer coefficient through wall
$\mathscr{U}_\mathrm{r}$	$1/\left(\frac{1}{h_\mathrm{a}}+\frac{\delta_\mathrm{r}}{k_\mathrm{r}}+\frac{1}{h_\mathrm{a}}\right)$	Overall heat transfer coefficient, room to ambient

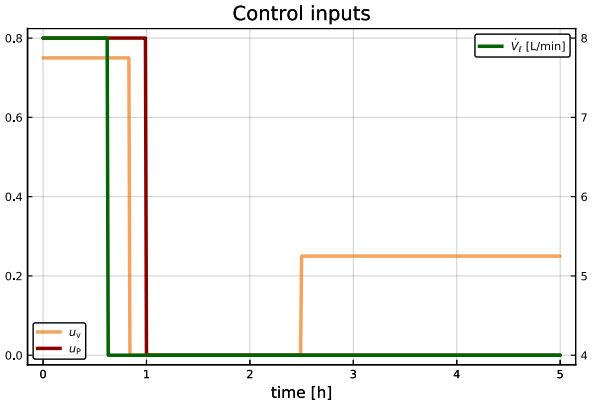

Figure 3. Control inputs u_P (power fraction to heated tank), u_v (water flow valve opening), and $\dot{V}_\ell$ (volumetric flow rate in heating loop).

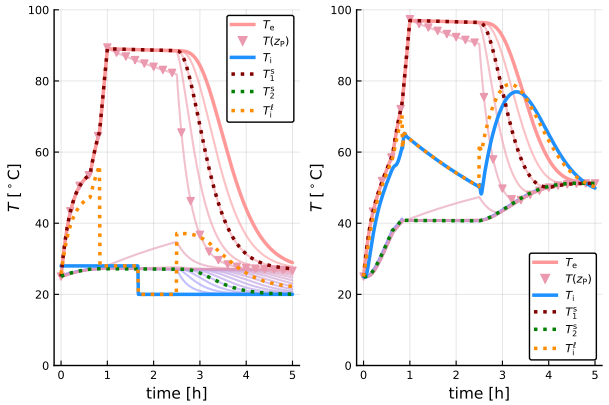

Figure 4. Temperature distribution (T_e: effluent temperture from heated tank; $T\,(z_\mathrm{P})$: temperature at heating element; T_i: influent temperature to heated tank; T_j^S temperature at heated tank sensors; T_i^ℓ inlet temperature to floor heating loop) in heated tank for cases (a) the heated tank is an independent system with specified tank inlet temperature T_i, and (b) the heated tank and the floor heating system are connected via a water loop where T_i is the return water temperature from the floor heating.

tank and the floor heating system are connected such that T_i is caused by a return of water from the floor.

Figure 5 shows the temperatures in the floor heating part: T_al, T_pq, T_r, T_fb, T_cb.

Using a DAE solver (OpenModelica), we immediately also find other quantities such as heat flows. As an example, Fig. 6 shows the heat flow from water pipe to aluminum, $\dot{Q}_\mathrm{al2p}$, as well as heat flow out of the aluminum plate, $\dot{Q}_\mathrm{al2x}$. Furthermore, the figure shows the separate heat flow from aluminum to parquet, $\dot{Q}_\mathrm{al2pq}$, and from aluminum to fiberboard, $\dot{Q}_\mathrm{al2fb}$.

Because steady state is assumed for the aluminum plate, $\dot{Q}_\mathrm{al2x} \equiv \dot{Q}_\mathrm{p2al}$. Furthermore, $\dot{Q}_\mathrm{al2x} = \dot{Q}_\mathrm{al2pq} + \dot{Q}_\mathrm{al2fb}$. Observe that with the given initial temperatures of the fiberboard, $\dot{Q}_\mathrm{al2fb} < 0$ in these operating conditions.

Figure 7 shows the total heat flow from the parquet to the room, and the heat flow due to convection vs. radiation.

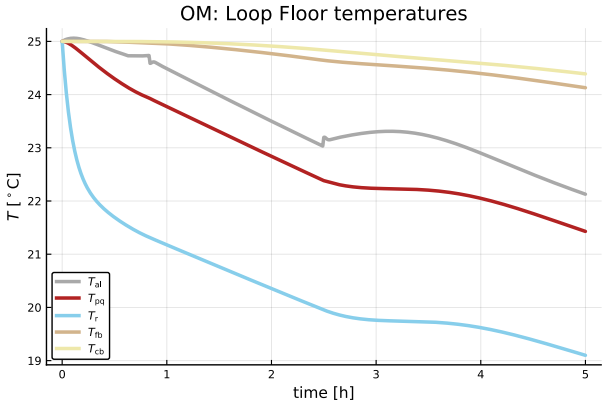

Figure 5. Temperature evolution in various compartments in the floor heating system (T_j: temperature in compartment j — al: aluminum plate, pq: parquet, r: room, fb: fiber board, cb: chip board). Observe that all compartments start at 25 °C.

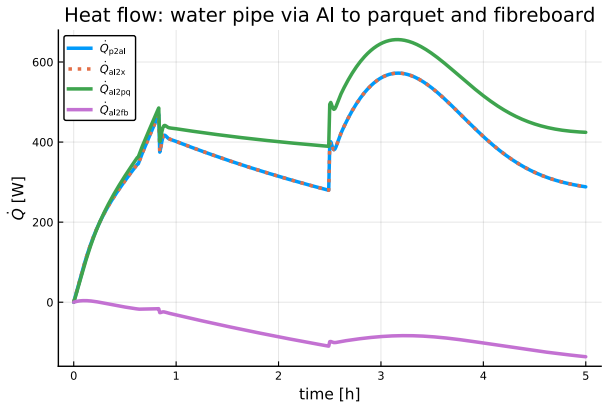

Figure 6. Heat flows from floor water pipe through aluminum to parquet and fiberboard ($\dot{Q}_{i2j}$: heat flow rate from compartment i to j, where i, j are p: water pipe, al: aluminum plate, pq: parquet, fb: fiber board). Observe that for the case studied here, the flow from the aluminum plate to the fibreboard is negative.

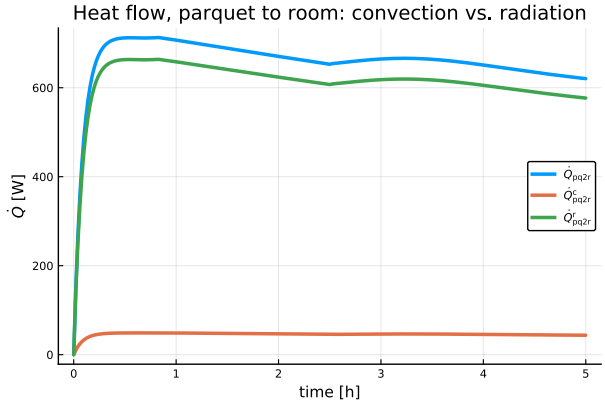

Figure 7. Heat flows from parquet to room ($\dot{Q}^k_{i2j}$: heat flow rate from compartment i to compartment j, where pq: parquet, r: room, and k indicates heat flow type, c: convection, r: radiation).

An interesting observation is that heat flow by radiation dominates over heat flow by convection. Often, the radiation flow term is linearized and converted into a quasi convection term, with modification of the total heat transfer coefficient.

5 Conclusions

A previous model of a stratified heated water tank has been improved, and extended with a water circulation loop for heating of the floor in a room. A simple approximation of an advection model has been used in the water loop, and the heat transfer to the floor layers has been described as a cross-current heat exchanger to an aluminum plate with infinitely fast dynamics. The heat is then transported from the aluminum plate to a chip-board below the aluminum plate, and through a fiberboard plate through the parquet, and then via convection and radiation to the room. In the floor layers, the effects of a thin plastic film and a thin felt paper have been neglected, and perfect insulation has been assumed below the chipboard. The room model is overly simple in that only air has been included; in reality, air heats furniture, walls, etc., which will add to the thermal mass of the room. Still, the extension in the paper are believed to give a realistic description of the transfer of heat from a heated tank to the floor of a building.

An important result is that the water circulation loop has a considerable effect on the dynamics of the water tank temperatures. A previous paper discussed tuning of parameters for model fitting. The effect of the circulation loop indicates that the circulation loop should be taken into consideration when tuning model parameters.

The model contains a large number of parameters; (Johansen et al., 2019) and Table 2. Most of these parameters are available from the literature/experimental work at building institutes. Because of the physical nature of the model, such literature values will not be too far off from their real values. However, some of the parameters are uncertain. This is especially true with some heat transfer coefficients. Thus, in practice, it will be necessary to tune some of the parameter values based on available experimental data. Because of the physical nature of the model, the model can be expected to generalize better to other buildings than a purely empirical/data-driven model would have.

Future work will include a more detailed room/apartment model, and better scaling of the heater power compared to the heat loss in the system. It is also of interest to include more formal description of water physics and heat transfer. Model fitting will be an important part of an improved model. Finally, it is of interest to look more into how such a model can be used in a control system.

References

Karl Johan Åstrøm and Richard M. Murray. *Feedback Systems. An Introduction for Scientists and Engineers*. Princeton University Press, Princeton, NJ, 2008. ISBN 978-0-691-13576-2.

S.Y. Ho, R.E. Hayes, and R.K. Wood. Simulation of the dynamic behaviour of a hydronic floor heating systems. *Heat Recovery Systems & CHP*, 15(6):505–519, 1995.

Casper Amandus Johansen, Bernt Lie, and Nils-Olav Skeie. Models for control of thermal energy in buildings. In Erik Dahlquist, Esko Juuso, Bernt Lie, and Lars Eriksson, editors, *Proceedings of the 60th Conference on Simulation and Modelling (SIMS 59)*, number 170 in Linköping Electronic Conference Proceedings. Linköping University Electronic Press, 2019. doi:https://doi.org/10.3384/ecp20170.

Jesus Lago, Fjo De Ridder, Wiet Mazairac, and Bart De Schutter. A 1-dimensional continuous and smooth model for thermally stratified storage tanks including mixing and buoyancy. *Applied Energy*, 248:640–655, 2019.

Bernt Lie. Improved model for solar heating of buildings. In Lena Buffoni, Adrian Pop, and Bernhard Thiele, editors, *Proceedings, The 56th Conference of Simulation and Modelling*, pages 299–308, Linköping University, Sweden, October 2015. Scandinavian Simulation Society, Linköping University Electronic Press. doi:10.3384/ecp15119, pp. 299–308. October 7–9 2015.

Bernt Lie, Carlos Pfeiffer, Nils-Olav Skeie, and Hans-Georg Beyer. Models for solar heating of buildings. In Alireza Rezania Kolai, Kim Sørensen, and Mads Pagh Nielsen, editors, *Proceedings, 55th International Conference of Scandinavian Simulation Society*, pages 28–38, Aalborg University, Denmark, October 2014. Scandinavian Simulation Society, Linköping University Electronic Press. doi:www.ep.liu.se/ecp/108/ecp14108.pdf. October 21–22 2014.

Aksel L. Lydersen. *Fluid Flow and Heat Transfer*. John Wiley & Sons, Chichester, 1979.

R. Viskanta, M. Behnia, and A. Karalis. Interferometric observations of the temperature structure in water cooled or heated from above. *Advances in Water Resources*, 1(2):57–69, 1977.

Evangelos Vrettos. *Control of Residential and Commercial Loads for Power System Ancillary Services*. PhD thesis, ETH, Power Systems Laboratory, 2016.

Zhijie Xu, Ruisheng Diao, Shuai Lu, Jianming Lian, and Yu Zhang. Modeling of electric water heaters for demand response: A baseline pde model. *IEEE Transactions on Smart Grid*, 5(5):2203–2210, September 2014. doi:10.1109/TSG.2014.2317149.